REVIEW

CLINICAL ANATOMY WILEY

Pediatric paranasal sinuses—Development, growth, pathology, & functional endoscopic sinus surgery

Sophie Lee[1] | Justin Fernandez[2] | S. Ali Mirjalili[1] | Joshua Kirkpatrick[1]

[1]Department of Anatomy and Medical Imaging, Faculty of Medical and Health Sciences, University of Auckland, Auckland, New Zealand

[2]Auckland Bioengineering Institute, University of Auckland, New Zealand

Correspondence
Joshua Kirkpatrick, Department of Anatomy and Medical Imaging, Faculty of Medical and Health Sciences, The University of Auckland, Auckland, New Zealand.
Email: jkir059@aucklanduni.ac.nz

Abstract

The paranasal sinuses (maxillary, frontal, ethmoid, and sphenoid sinuses) are complex anatomical structures. The development and growth of these have been investigated utilizing a number of different methods ranging from cadaveric analysis to modern cross sectional imaging with 3D modeling. An understanding of normal pediatric paranasal sinus embryology and development enables us to better determine when pathology may be affecting the normal developmental process. Cystic fibrosis, chronic sinusitis, deviated nasal septum and cleft lip and palate are some of the conditions which have been shown to effect paranasal sinus development to varying degrees. Functional endoscopic sinus surgery (FESS) is becoming increasingly common and an understanding of sinus anatomy together with when periods of rapid growth occur during childhood is important clinically. Although concerns have been raised regarding the impact of FESS on facial growth, there is limited evidence of this in regards to either changes in anthropomorphic measurements or clinical assessments of symmetry post operatively.

KEYWORDS
anatomy, embryology, ethmoid, frontal, functional endoscopic sinus surgery, maxillary, pediatric paranasal sinuses, sphenoid

1 | INTRODUCTION

It is important to understand the developmental anatomy of the paranasal sinuses in children (Figure 1). This is because accurate knowledge of sinus growth patterns is vital to our ability to diagnose pathology and plan appropriate treatment. These paired paranasal sinuses arise from the cartilaginous nasal capsule and develop with unique and highly variable growth patterns (Wang et al., 1994). This has important implications for surgical intervention—especially with the increasing use of functional endoscopic sinus surgery (FESS) (Vaid & Vaid, 2015). In this review, we will focus on the development of each of the paranasal sinuses, their normal growth pattern in

healthy children and how various pathological conditions or surgical trauma may influence this growth.

2 | METHODS

A systematic review of studies describing the developmental growth of the paranasal sinuses in children was conducted using MEDLINE, Scopus and Google Scholar (Figure 2). Bibliographies were reviewed to gain secondary references and textbook references were used to clarify points and controversies. Included studies were human based and written in the English language.
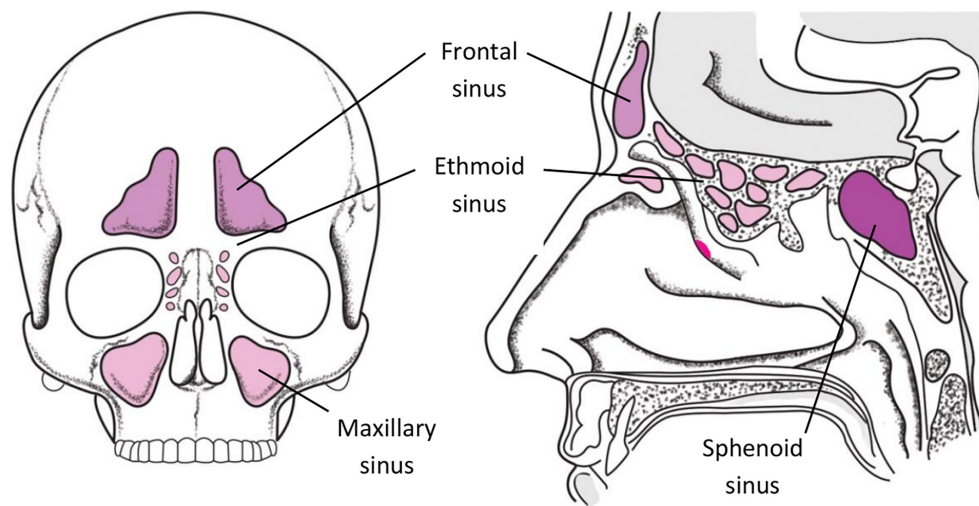
2.1 | Analyzing papers which analyze paranasal sinuses

This article aims to combine the breadth of research currently available on paranasal sinuses and their development. The studies included have utilized different methods which have varying degrees of accuracy, ranging from direct measurements on cadavers or skulls through to x-ray and cross sectional imaging with both CT and MRI. Even within the cross sectional imaging however factors such as the slice thickness effects accuracy as well as how the images are analyzed. Some studies use cross sectional imaging to calculate dimensions and then use rudimentary volumetric equations to estimate volume, others use automatic segmentation software to generate 3D models, the gold standard however is to manually segment osseous boundaries to generate 3D models. Factors which can make direct comparisons difficult between studies include: 1) Differences where measurements are taken from. Studies often do not specifying whether measurements are taken from the mucosal lining or bony surface of the sinus. 2) Underlying population and ethnic differences. 3) Analyzing populations in different age groups. Age groups may be particularly important if a period of rapid growth occurs during development. 4) Studies with low numbers as their mean will be disproportionately affected by outliers. These factors, namely the method used, study population, age groups and number of participants has been included in the reference tables to assist in analysis.

3 | MAXILLARY SINUS

The maxillary sinus (MS) is the largest of the four paranasal sinuses and is an air-filled, pyramidal-shaped cavity within the maxilla on either side of the nasal cavity with an apex extending into the zygomatic process. Boundaries of the sinus include the maxilla (anterolaterally), the anterior wall of the pterygopalatine fossa (posteriorly), the lateral wall of the nasal cavity (medially), the alveolar process (inferiorly) and the orbital floor (superiorly) (Lund et al., 2014; Zalzal
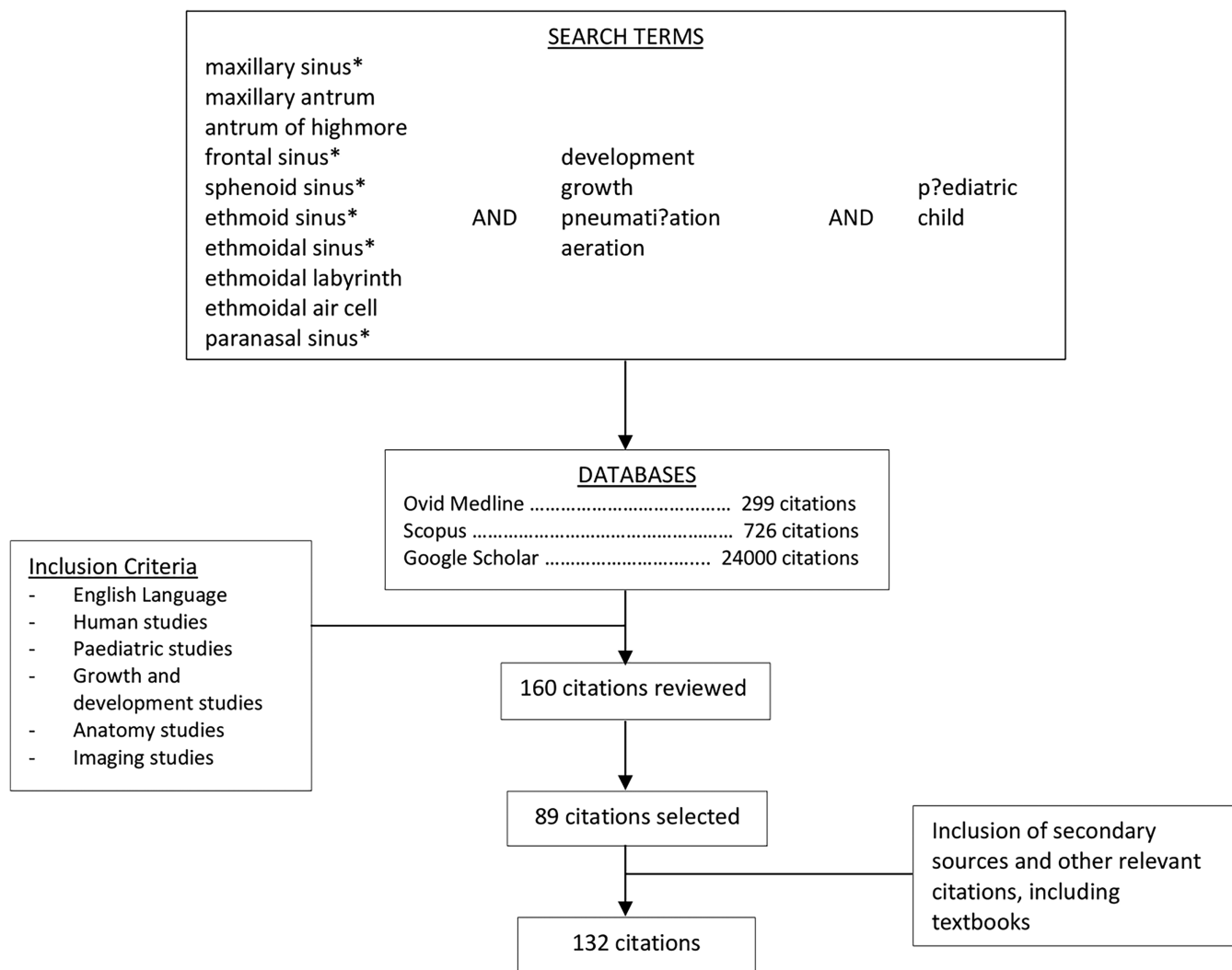
et al., 2018). The maxillary ostium is located at the superior aspect of the medial wall with secretions draining into the ethmoidal infundibulum and then on to the semilunar hiatus and into the middle meatus (Kubal, 1998; Lund et al., 2014).

3.1 | Maxillary sinus development

The MS is the first paranasal sinus to begin development, starting in the third gestational month. At 11–12 weeks, the primordial ethmoidal infundibulum begins developing lateral to the uncinate process in the middle meatus, and from here a channel develops infero-laterally toward the precursor of the maxillary bone. This forms the primordial maxillary sinus (Bingham et al., 1991). The MS gradually expands with progressive resorption of the surrounding nasal capsule and extends into the ossifying maxilla by 20 weeks of gestation (Anon et al., 1996; Ozcan et al., 2014). Growth occurs in all directions, with anterior–posterior expansion being the most marked, resulting in an elongated oval shape (Iwanaga et al., 2019).

The MS is filled with amniotic fluid during prenatal development and becomes aerated postnatally. This prenatal fluid content allows magnetic resonance imaging detection of fetal maxillary sinuses from the 22nd gestational week (Ozcan et al., 2014). Early postnatal radiographs suggested that the MS becomes fully aerated between 1 and 6 months of life (Maresh & Washburn, 1940; Walter, 1933). More recent studies however have suggested that this occurs over a much wider time interval and that there are relatively high rates of maxillary sinus opacification even in healthy children, with one study showing approximately 50% of children less than 13 years old have some degree of sinus opacification (Diament et al., 1987; Glasier et al., 1989). It has been hypothesized that this opacification may be a result of normal redundant mucosa, an abundance of tears or an easily occluded ostia (Diament et al., 1987; Glasier et al., 1989).

The morphological shape of the MS changes with age. When viewed anteriorly, the most common shaped is the rectangle from 1 to 3 years, the triangle from 4 to 12 years, and the upside-down

SEARCH TERMS

maxillary sinus*
maxillary antrum
antrum of highmore
frontal sinus*   development
sphenoid sinus*   growth   p?ediatric
ethmoid sinus*   AND pneumati?ation   AND   child
ethmoidal sinus*   aeration
ethmoidal labyrinth
ethmoidal air cell
paranasal sinus*

DATABASES
Ovid Medline ………………………………… 299 citations
Scopus ……………………………………………. 726 citations
Google Scholar …………………………….. 24000 citations

Inclusion Criteria
-    English Language
-    Human studies
-    Paediatric studies
-    Growth and
     development studies
-    Anatomy studies
-    Imaging studies

160 citations reviewed

89 citations selected

Inclusion of secondary
sources and other relevant
citations, including
textbooks

132 citations

FIGURE 2   Literature search strategy for reports of paranasal sinus development in children. *Google scholar search limited to first 30 pages (300 hits)

triangle shape from age 13 onwards (Rennie et al., 2017a). On the lateral view, the MS is quadrilateral across all the age groups with differences only noted along the inferior wall of the sinus which is influenced by teeth eruption. Studies generally report symmetrical growth of the maxillary sinus' throughout childhood (Adibelli et al., 2011; Barghouth et al., 2002; Bhushan et al., 2016; Degermenci et al., 2016; Lee et al., 2020; Lorkiewicz-Muszynska et al., 2015; Park et al., 2010; Rennie et al., 2017b; Smith et al., 2017).

3.2 | Maxillary sinus size and growth

A number of studies have recorded MS growth throughout childhood and adolescence, providing data that can be used as a reference for normal growth (Tables 1 and 2). The MS is approaching its adult size by 15–18 years of age, however growth does not stop until the third decade of life (Figure 3) (Ikeda et al., 1998; Jun et al., 2005; Karakas & Kavakli, 2005; Sánchez Fernández et al., 2000). A large MRI study

($n = 1383$) showed that at birth the MS measures approximately $7 \times 4 \times 3$ mm ($l \times h \times w$) and this increased to $34 \times 32 \times 28$ mm by 15–18 years of age (Adibelli et al., 2011). A study utilizing automatic 3D segmentation demonstrated a MS volume at 1 to 3 years of approximately 1.6 cm^3, this increased to 12.6 cm^3 by 22–25 years (Rennie et al., 2017b). Ethnic differences in sinus volume have also been reported (Rennie et al., 2017b). A New Zealand study (CT, $n = 65$) using manual segmentation performed a linear regression analysis and estimated an average two yearly growth of 2.54 cm^3 (Lee et al., 2020). There is some evidence that MS growth is similar in males and females during childhood, but during the late teenage years sexual dimorphism becomes apparent (Lorkiewicz-Muszynska et al., 2015; Rennie et al., 2017b). This is supported by adult studies which confirm larger maxillary sinuses in males (Amin & Hassan, 2012; Ekizoglu et al., 2014; Fernandes, 2004).

It is widely believed that the MS demonstrates biphasic rapid growth during the first 4 to 5 years of life and then again from 8 years, with relatively slow growth in the interim (Chang et al., 2014;

TABLE 1 Previous studies analyzing MS dimensions in children—length (anterior–posterior), height (cranio-caudal), and width (transverse)

Author	Sample size (n)	Age (years)	Population	Methodology	Mean measurements from youngest age group studied (mm)			Mean measurements from oldest age group studied (mm)		
					Length	Height	Width	Length	Height	Width
Weiglein et al., 1992	134	0–12	Austria	Dried skulls	8–13 (age 0)	3–4 (age 0)	3–5 (age 0)	35–40 (age 12)	22–28 (age 12)	20–29 (age 12)
Wolf et al., 1993	102	0–12	Austria	Dried skulls + cadavers	10 (age 0)	4 (age 0)	3 (age 0)	34–38 (age 4–8)	22–26 (age 4–8)	18–24 (age 4–8)
Schaeffer, 1936	Not stated	0–18	USA	Cadavers	7–8 (at birth)	4–6 (at birth)	3–4 (at birth)	31–33 (age 18)	20–21 (age 18)	19–21 (age 18)
Robinson et al., 1982	24 normal controls	0–19	USA	X-ray	26 (age 0)	10 (age 0)	—	41 (age 19)	33 (age 19)	—
Bhushan et al., 2016	139	0–18	USA	CT	R: 25.1 L: 24.3 (age < 6)	R: 17.8 L: 17.6 (age < 6)	R: 16.5 L: 16 (age < 6)	R: 36 L: 36.7 (age > 12)	R: 35.6 L: 35.8 (age > 12)	R: 24.6 L: 24.9 (age > 12)
Sánchez Fernández et al., 2000	100 normal controls	1–88	Spain	CT	16 (age 1–5)	—	8 (age 1–5)	26 (age > 20)	—	18.7 (age > 20)
Lorkiewicz-Muszynska et al., 2015	170	1–17	Poland	CT	F: 14.4 M: 10.4 (age 1)	F: 5.8 M: 4.3 (age 1)	F: 7.1 M: 4.3 (age 1)	F: 40 M: 38.8 (age 17)	F: 27.5 M: 30.2 (age 17)	29.5 (age 17)
Degermenci et al., 2016	361	0–18	Turkey	CT	R: 13.3 L: 13.4 (age 1)	R: 11 L: 11.1 (age 1)	R: 8.4 L: 8.8 (age 1)	33.6 (age 18)	R: 33.5 L: 34.7 (age 18)	R: 21.4 L: 22.2 (age 18)
Lee et al., 2020	65	0–18	New Zealand	CT	9.4 (0–1)	12.5 (0–1)	16.5 (0–1)	43.0 (16–18)	46.3 (16–18)	33.9 (16–18)
Adibelli et al., 2011	1383	0–18	Turkey	MRI	6.9 (age 0–2.9 mo)	4.1 (age 0–2.9 mo)	2.6 (age 0–2.9 mo)	34.2 (age 15–18)	31.8 (age 15–18)	28.1 (age 15–18)
Barghouth et al., 2002	179	0–17	Switzerland	MRI	7.3 (at birth)	4 (at birth)	2.7 (at birth)	38.8 (age 16)	36.3 (age 16)	27.5 (age 16)

TABLE 2   Previous studies analyzing maxillary sinus volumes in children

Author	Sample size (n)	Age (years)	Population	Methodology	Mean volumes from youngest age group studied (cm^3)	Mean volumes from oldest age group studied (cm^3)
Barghouth et al., 2002	179	0–17	Switzerland	MRI, volume via ellipsoidal formula $V = \frac{1}{2} \times A \times B \times C$	0.08 (at birth)	18.3 (age 16)
Adibelli et al., 2011	1383	0–18	Turkey	MRI, volume via ellipsoidal formula	0.16 (age 0–2.9 mo)	23.65 (age 15–18)
Degermenci et al., 2016	361	0–18	Turkey	CT, volume via ellipsoid formula & analysis with Cavalieri's principle	0.95 (R), 0.98 (L) (age 1)	12.74 (R), 13.54 (L) (age 18)
Bhushan et al., 2016	139	0–18	USA	CT, volume via rectangular formula length × width × height	8.76 (R), 8.12 (L) (age < 6)	33.16 (R), 34.14 (L) (age > 12)
Lorkiewicz-Muszynska et al., 2015	170	0–18	Poland	CT, volume via average of pyramid & sphere volumes	F: 0.36, M: 0.1 (age 1)	F: 13.2, M: 15.17 (age 17)
Ikeda et al., 1998	20 normal controls	4–79	Japan	CT, volume via trapezoidal formula $V = \frac{(A1+A2)h}{2} + \frac{(A2+A3)h}{2} +$	11.0 (age 4–9)	20.5 (age ≥ 15)
Sánchez Fernández et al., 2000	100 normal controls	1–88	Spain	CT, volume via with trapezoidal formula	0.6 (age 1–5)	13.07 (age > 20)
Karakas & Kavakli, 2005	91	5–55	Turkey	CT, volume calculated with Cavalieri's principle	F: 7.03 (R), 6.6 (L) M: 5.34 (R), 6.7 (L) (age 5–10)	F: 11.13 (R), 11.53 (L) M: 15.04 (R), 15.97 (L) (age > 25)
Jun et al., 2005	173	0–80	Korea	HRCT images (2.5 mm slice thickness), 3D automatic reconstruction	7.38 (age 0–10)	18.67 (age 21–30)
Park et al., 2010	260	0–25	Korea	HRCT images (1 mm slice thickness), 3D automatic reconstruction	0.75 (age 0)	14.78 (age 25)
Smith et al., 2017	32	6–18	USA	CBCT, 3D manual reconstruction	4.8 (age 6)	17.37 (age 18)
Rennie et al., 2017b	480	1–25	South Africa	CT (0.625–1.25 mm slice thickness), automatic 3D reconstruction	1.61 (R), 1.57 (L) (age 1–3)	12.58 (R), 12.64 (L) (age 22–25)
Lee et al., 2020	65	0–18	New Zealand	CT (<3 mm slice thickness) 3D manual reconstruction	0.81 (0–1)	21.63 (age 16–18)

Cunningham et al., 2016; Lee et al., 2020). The first growth spurt is more significant with volume increasing by >750%, the second phase of increased growth is slower with volume increasing by 186% (Lee et al., 2020). Some authors disagree with the biphasic model however, claiming that after the early phase of growth there is ongoing slow growth thereafter (Adibelli et al., 2011; Barghouth et al., 2002; Lorkiewicz-Muszynska et al., 2015). Differences in definition of rapid growth and age brackets used (some up to 6 years) likely contribute to differences reported. An understanding of these periods of rapid growth is essential as it may determine if a child needs repeat imaging prior to surgery (Shah et al., 2003). During the first growth spurt, the sinus reaches the infraorbital canal laterally and the attachment of the inferior turbinate inferiorly (Iwanaga et al., 2019; Zeifer, 2000). Further lateral expansion passes the infraorbital canal by 4 to 8 years,

and during the second period of increased growth, it expands to the molar teeth and reaches the zygomatic recess by 12 years of age (Ogle et al., 2012; Wolf et al., 1993). Inferior growth reaches the midportion of the inferior meatus by age 7, the plane of the hard palate by age 9, becoming level with the nasal floor by age 12 and ultimately slowly descending in the early twenties approximately 5 mm below the level of the nasal floor following the eruption of the adult molars (Scuderi et al., 1993).

4 | FRONTAL SINUS

The frontal sinuses (FS) are paired, pyramidal shaped cavities located posterior to the superciliary arches between the anterior and
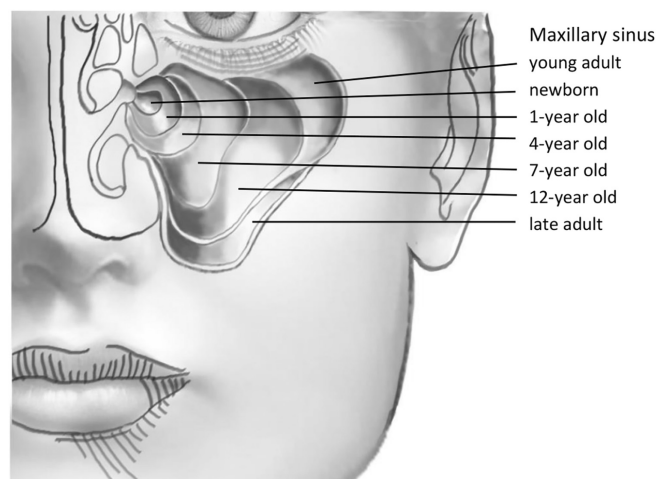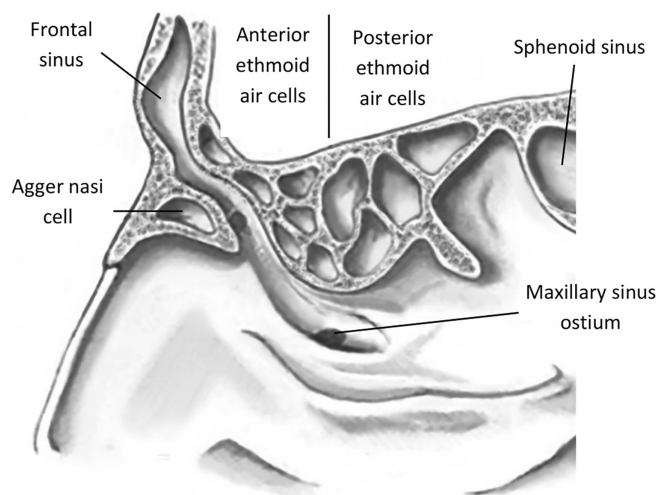
FIGURE 3 Maxillary sinus development with age

FIGURE 4 Frontal and ethmoid sinuses

posterior tables of the frontal bone (Duque & Casiano, 2005; Lund et al., 2014). The floor of the sinus is formed by the roof of the orbit and they are separated from each other by an intersinus septum (McLaughlin Jr et al., 2001). Drainage occurs through the posteromedial aspect of the sinus floor via the FS outflow tract (Parikh & Brown, 2004; Zalzal et al., 2018). Secretions pass down the frontal infundibulum through the narrow frontal ostium and enter the frontal recess forming a narrow cleft within the anterior ethmoidal cells which widens inferiorly and posteriorly to drain into the middle meatus (Figure 4) (Friedman et al., 2004). The anatomy of the frontal recess is complex and is determined by a number of surrounding structures and anatomic variants including the agger nasi, frontal cells and anterior ethmoidal cells (Friedman et al., 2004). These adjacent structures can compromise the patency of the frontal recess, making this location responsible for most cases of frontal sinusitis. It also makes FESS very challenging (McLaughlin Jr et al., 2001).

4.1 | Frontal sinus development

The frontal sinuses are the last of the paranasal sinuses to develop occurring during the third or fourth month of fetal life. They begin as an outpouching of the lateral nasal wall, at the level of the anterosuperior portion of the middle nasal meatus. This outpouching then extends superomedially giving origin to the ethmoidal cells and the frontal recess (Marciniak & Nizankowski, 1959). In the majority of cases, the frontal sinus arises from rudiments in the frontal recess but other possible origins include the anterior ethmoidal cells, the ethmoidal infundibulum, the suprabullar recess or a combination of these. This results in highly variable nasofrontal connections and a complex drainage system (Lund et al., 2014; Schaeffer, 1936).

The FS begins pneumatizing the horizontal plate of the frontal bone at 1 to 2 years and advances superiorly to above the anterior ethmoidal cells at the level of the nasion by 3 years (Davis, 1918). At 4 to 7 years it reaches the level of the orbital roof and becomes

radiographically visible in the majority of children, before pneumatizing the vertical plate of the frontal bone (Adibelli et al., 2011; Barghouth et al., 2002; Moore & Ross, 2017; Parikh & Brown, 2004; Sardi et al., 2018; Scuderi et al., 1993; Yun et al., 2011). The extent which FS pneumatization occurs is highly variable and can range from complete absence to hyperpneumatization which has been shown to advance into the sphenoid wings, parietal, maxilla or temporal bones (Al-Bar et al., 2015). One adult study reported that the most common shape of the FS is quadrangular when viewed anteriorly (43.9%) and concave when viewed laterally (46.5%) (Kim et al., 2013). No similar studies have been conducted in children however, and so how these shapes develop in childhood remains unclear.

Asymmetry of the frontal sinuses has been documented with the left sinus tending to be larger (Aslier et al., 2016; Hacl et al., 2017; Kanat et al., 2015; Kim, 1962; Rennie et al., 2017b; Rubira-Bullen et al., 2010; Spaeth et al., 1997; Tatlisumak et al., 2017; Yoshino et al., 1987). One study documented asymmetry in 86% of individuals with the left sinus being larger in 59% of asymmetrical cases (Kanat et al., 2015). This may be partially explained by the fact that the left sinus continues to grow until 25 years of age, while the right generally stops at 16–18 years (Rennie et al., 2017b). Unilateral FS aplasia occurs in approximately 5% of adults with bilateral aplasia occurring in 4% (Zalzal et al., 2018). FS aplasia rates depends on the climate and population studied with Canadian Inuit reporting rates of up to 43% for bilateral FS aplasia (Tatlisumak et al., 2008).

4.2 | Frontal sinus size and growth

A number of studies have attempted to calculate growth patterns of the FS throughout childhood recording both linear dimensions and volumes (Tables 3 and 4). The height or width is generally the largest dimensions, with the anterior–posterior length being the smallest (Adibelli et al., 2011; Barghouth et al., 2002; Schaeffer, 1936; Weiglein et al., 1992; Wolf et al., 1993; Yun et al., 2011). A Turkish

TABLE 3 Previous studies that have analyzed FS measurements in children

Author	Sample size (n)	Age (years)	Population	Methodology	Mean measurements from youngest age group studied (mm)			Mean measurements from oldest age group studied (mm)		
					Length	Height	Width	Length	Height	Width
Schaeffer, 1936	Not stated	0–20	USA	Cadavers	3.5 (age 6–12 months)	2 (age 6–12 months)	2 (age 6–12 months)	17 (age 19–20)	26 (age 19–20)	26 (age 19–20)
Weiglein et al., 1992	134	0–12	Austria	Dried skulls	7–13 (age 4)	4–9 (age 4)	4–10 (age 4)	13–21 (age 12)	12–26 (age 12)	15–22 (age 12)
Wolf et al., 1993	102	0–12	Austria	Dried skulls & cadavers	4–8 (age 1–4)	6–9 (age 1–4)	4–7 (age 1–4)	6–10 (age 4–8)	15–16 (age 4–8)	8–10 (age 4–8)
Valverde et al., 2013	20	7–17	Japan	Lateral X-ray	—	—	7.15 (age 8)	—	—	10.78 (age 17)
Gagliardi et al., 2004	31	7–18	Aboriginal Australians	Lateral X-ray	7.2 (M) 8.1 (F) (age 8)	15.3 (M) 12.4 (F) (age 8)	—	20.5 (M) 17.1 (F) (age 18)	36.9 (M) 40.2 (F) (age 18)	—
Spaeth et al., 1997	5600	0–25	Germany	CT of skulls	7.83 (M) 11.67 (F) (age 6)	—	11.92 (M) 11.58 (F) (age 6)	17.38 (M) 16.11 (F) (age 25)	—	27.98 (M) 26.39 (F) (age 25)
Sánchez Fernández et al., 2000	100	1–88	Spain	CT	7 (age 6–10)	—	7 (age 6–10)	13 (age > 20)	—	18 (age > 20)
Yun et al., 2011	352	1–23	Korea	CT, 3D reconstruction	2.3 (age 4)	1.8 (age 4)	4.1 (age 4)	21.6 (age 20)	27.9 (age 20)	52.8 (age 20)
Barghouth et al., 2002	12	0–17	Switzerland	MRI	—	—	—	12.8 (age 16)	21.9 (age 16)	24.5 (age 16)
Adibelli et al., 2011	612	0–18	Turkey	MRI	3.5 (age 3–5.9)	5.2 (age 3–5.9)	4.8 (age 3–5.9)	16.6 (age 15–18)	36.9 (age 15–18)	38.3 (age 15–18)

TABLE 4 Previous studies that have analyzed FS volume in children

Author	Sample size (n)	Age (years)	Population	Methodology	Mean volumes from youngest age group (cm³)	Mean volumes from oldest age group (cm³)
Sánchez Fernández et al., 2000	100	1–88	Spain	CT, volume via trapezoidal formula $V = \frac{(A1+A2)h}{2} + \frac{(A2+A3)h}{2} +$	0.7 (age 6–10)	3.7 (age > 20)
Karakas & Kavakli, 2005	91	5–55	Turkey	Axial CT, volume calculated with Cavalieri's principle	F: 1.23 M: 1.19 (age 5–10)	F: 3.5 M: 8.41 (age > 25)
Rennie et al., 2017a, 2017b, 2017c	480	1–25	South Africa	Axial CT (0.625–1.25 mm slice thickness), 3D reconstruction	0.49 (R) 0.44 (L) (age 1–3)	4.76 (R) 4.31 (L) (age 22–25)
Park et al., 2010	260	0–25	Korea	CT, 3D reconstruction, automatic volume calculation	0.003 (age 2)	3.764 (age 25)
Yun et al., 2011	352	1–23	Korea	CT, 3D reconstruction, automatic volume calculation	0.07 (R) 0.11 (L) (age 4)	3.9 (R) 4.5 (L) (age 20)
Adibelli et al., 2011	612	0–18	Turkey	MRI, volume via ellipsoidal formula $V = \frac{1}{2} \times A \times B \times C$	0.25 (age 3–5.9)	6.28 (age 15–18)

study (MRI, $n = 612$) first observed the FS at 3 to 6 years with an average size of $3.5 \times 5.2 \times 4.8$ mm ($l \times h \times w$), this increased to $16.6 \times 36.9 \times 38.3$ mm by 15–18 years (Adibelli et al., 2011). One 3D reconstructive study (CT, $n = 480$) found that the volume of the FS in children 1 to 3 years of age was approximately 0.5 cm³ which increased to approximately 4.5 cm³ by 22–25 years (Rennie et al., 2017b). There is a large amount of variability even using cross sectional imaging and the large standard deviations demonstrate significant variation within populations.

A period of accelerated FS growth has been identified between 13 and 16 years of age approximately 1.4 years after the pubertal growth spurt (Gagliardi et al., 2004; Ruf & Pancherz, 1996; Valverde et al., 2013; Yun et al., 2011). It is not clear what triggers this but some have speculated that it may be associated with the phases of craniofacial growth or hormonal changes during puberty (Duque & Casiano, 2005; Moore & Ross, 2017). The FS generally reaches full maturity between 20 and 25 years of age (Karakas & Kavakli, 2005; Rennie et al., 2017b; Yun et al., 2011). Sexual dimorphism has been demonstrated with males estimated to have a FS 13%–17% larger between 0 and 25 years of age, male FS may also continue growing for longer than females (Adibelli et al., 2011; Brown et al., 1984; Karakas & Kavakli, 2005; Prossinger, 2001; Rennie et al., 2017b; Spaeth et al., 1997).

5 | THE SPHENOID SINUS

The sphenoid sinuses (SS) are cuboidal in shape, positioned within the sphenoid bone and are the most posterior of the paranasal sinuses. The boundaries of the SS are the ethmoidal cells anteriorly, the clivus posteriorly and the intersinus septum medially (Anusha et al., 2014; Schaeffer, 1920; Wang et al., 2010). The sphenoid ostium is within its anterior wall and drains into the spenoethmoidal recess which is continuous with the superior nasal meatus (Anusha et al., 2014; Zeifer, 2000).

5.1 | Sphenoid sinus development

Development of the SS begins in the third month of gestation as an invagination of the nasal mucosa into the posterior portion of the cartilaginous nasal capsules. This results in the formation of a pouch like primitive sinus (Fujioka & Young, 1978). In the fifth month the anterolateral walls begin ossifying to form the sphenoidal conchae (Davis, 1918). The progressive postero-inferior expansion continues and at 3 years of age it fuses with the sphenoid bone (Van Alyea, 1941). The sinus extends inferiorly to the pterygoid canal by 6 to 7 years, posteriorly to the hypophyseal fossa by 8 years, laterally toward the anterior clinoid process by 8 to 12 years and then on toward the optic strut (Shah et al., 2003; Weiglein et al., 1992). Medial expansion also occurs resulting a in a progressive thinning of the intersinus septum (Van Alyea, 1941).

Once the SS extends into the presphenoidal plate, pneumatization proceeds in an inferior and posterior-lateral direction (Anusha et al., 2014). The age at onset of SS pneumatization is variable and although it has been demonstrated to occur in newborns, most studies generally agree that the majority of individuals have detectable pneumatization by 3 to 5 years (Barghouth et al., 2002; Fujioka & Young, 1978; Jang & Kim, 2000; Reittner et al., 2001; Rennie et al., 2017b; Szolar et al., 1994; Vidić, 1968). The extent of pneumatization can be described based on its position relative to the sella turcica (Hammer & Rådberg, 1961). The conchal type, generally occurs in 1 to 3 year olds with pneumatization only extending posteriorly to the plane of fusion of the sphenoidal conchae and the body of

the sphenoid bone (Hammer & Rådberg, 1961; Rennie et al., 2017c). The presellar type, which dominates in 4 to 9 year olds, and the sellar types, which dominate beyond 10–12 years, occur when the extent of pneumatization extends to a point either anteriorly or posteriorly to a vertical line drawn through the tuberculum sellae respectively (Figure 5) (Anusha et al., 2014; Rennie et al., 2017c). This distinction is important when considering transsphenoidal surgery as the conchal form makes this approach more technically difficult (Rennie et al., 2017c; Wang et al., 2010). Anteriorly the SS progresses from a small oval or cuboidal shape to a larger quadrilateral shape as lateral expansion occurs. The extent of pneumatization is variable and effects the sinus morphology with the pentagon shape being associated with pneumatization into the greater wings of the sphenoid and hexagonal shapes being associated with pneumatization of the pterygoid plate (Jaworek-Troć et al., 2021; Rennie et al., 2017c).

The sphenoid sinus is surrounded by a number of critical anatomical structures including both the pituitary and middle cranial fossa's superiorly and the cavernous sinus laterally (Anusha et al., 2014; Lund et al., 2014). Depending on the extent of pneumatization a number of neurovascular structures may form bony prominences or recesses within the SS with only a thin plate of bone for protection. These include the optic nerve superolaterally, the internal carotid artery posterolaterally, and the maxillary nerve inferiorly (Anusha et al., 2014). These anatomic relations are important clinically as sinusitis can spread and potentially result in meningitis, an intracranial abscess, or cavernous sinus thrombosis, they can also potentially be damaged during FEES with significant sequelae (Reittner et al., 2001; Štoković et al., 2016).

5.2 | Sphenoid sinus size and growth

Multiple studies have analyzed the increasing size and volume of the SS with age (Tables 5 and 6). A Turkish MRI study ($n = 876$) demonstrated an average sinus sizes of $4.6 \times 4.1 \times 3.9$ mm ($l \times h \times w$) at 1 to 3 years of age increasing to $29.7 \times 27.6 \times 23.2$ mm at 12–14.9 years (Adibelli et al., 2011). One Korean study (MRI, $n = 260$) utilizing a 3D segmented model showed volumes of 0.018 cm^3 at 1 year of age, increasing to 3.418 cm^3 by 25 years of age (Park et al., 2010). Periods of accelerated growth have been recorded as occurring prior to 5 years of age and also between the ages of 6 and 10 (Park
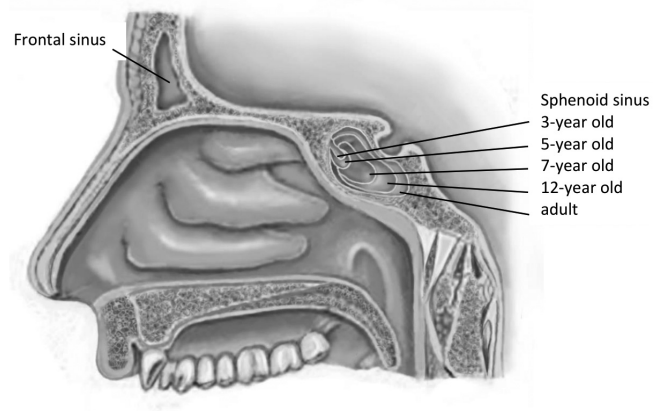

FIGURE 5 Sphenoid sinus development with age

TABLE 5 Previous studies that have analyzed sphenoid sinus measurements in children

Author	Sample size (n)	Age (years)	Population	Methodology	Mean measurements of youngest age group studied (mm)			Mean measurements of oldest age group studied (mm)		
					Length	Height	Width	Length	Height	Width
Schaeffer, 1936	Not stated	1–14	USA	Cadavers	1.5 (age 1)	2.5 (age 1)	2.5 (age 1)	12 (R), 7 (L) (age 14)	14 (R), 15 (L) (age 14)	9 (R), 14 (L) (age 14)
Wolf et al., 1993	102	0–12	Austria	Dried skulls + cadaver heads	4–6 (age 1–4)	3–5 (age 1–4)	6–8 (age 1–4)	11–14 (age 4–8)	7–11 (age 4–8)	9–11 (age 4–8)
Weiglein et al., 1992	134	0–12	Austria	Dried skulls	4–6 (age 4)	3–5 (age 4)	6–8 (age 4)	12–20 (age 12)	9–16 (age 12)	10–18 (age 12)
Sánchez Fernández et al., 2000	100 normal controls	1–88	Spain	CT	13 (age 6–10)	—	9 (age 6–10)	18 (age > 20)	—	15 (age > 20)
Spaeth et al., 1997	5600	0–25	Germany	CT	6.82 (M) 9.33 (F) (age 3)	—	6.42 (M) 8.77 (F) (age 3)	32.91 (M) 27.96 (F) (age 25)	—	33.45 (M) 32.78 (F) (age 25)
Barghouth et al., 2002	95	0–17	Switzerland	MRI	5.8 (age 3)	8.0 (age 3)	5.8 (age 3)	23 (age 16)	22.6 (age 16)	12.8 (age 16)
Szolar et al., 1994	401	0–15	Austria	MRI	6.2 (age 1–2)	6 (age 1–2)	7.4 (age 1–2)	22.1 (age 13–14)	20.6 (age 13–14)	26.5 (age 13–14)
Reittner et al., 2001	800	0–14	Austria	MRI	8.4 (age 1–2)	10.2 (age 1–2)	6.2 (age 1–2)	29.1 (age 14–15)	26.8 (age 14–15)	29.6 (age 14–15)
Adibelli et al., 2011	876	0–18	Turkey	MRI	0.35 (age 6–8.9 mo)	0.37 (age 6–8.9 mo)	0.33 (age 6–8.9 mo)	32.0 (age 15–18)	28.1 (age 15–18)	23.8 (age 15–18)

TABLE 6 Previous studies that have analyzed volumetric growth of the sphenoid sinus in children

Author	Sample size (n)	Age (years)	Population	Methodology	Mean volume youngest age cohort (cm^3)	Mean volume oldest age cohort (cm^3)
Karakas & Kavakli, 2005	91	5–55	Turkey	CT, volume calculated with Cavalieri's principle	2.96 (M) 3.14 (F) (age 5–10)	8.53 (M) 7.88 (F) (age > 25)
Sánchez Fernández et al., 2000	100 normal controls	1–88	Spain	CT, volume calculated with trapezoidal rule	1.5 (age 1–5)	3.5 (age > 20)
Park et al., 2010	260	0–25	Korea	CT, 3D reconstruction	0.018 (age 1)	3.418 (age 25)
Rennie et al., 2017a, 2017b 2017c	480	1–25	South Africa	CT, 3D reconstruction	0.1966 (R) 0.2729 (L) (age 1–3)	4.584 (R) 4.735 (L) (age 22–25)
Barghouth et al., 2002	95	0–17	Switzerland	MRI, sinus volume index calculated with ellipsoidal formula	—	2.7 (age 16)
Adibelli et al., 2011	876	0–18	Turkey	MRI, sinus volume index calculated with ellipsoidal formula	0.004 (age 6–8.9 mo)	4.96 (age 15–18)

et al., 2010; Shah et al., 2003). The majority of growth has occurred by 14–16 years of age (Barghouth et al., 2002; Hinck & Hopkins, 1960; Karakas & Kavakli, 2005; Park et al., 2010; Rennie et al., 2017b; Sánchez Fernández et al., 2000; Spaeth et al., 1997; Yonetsu et al., 2000). Left–right asymmetry is common however there is no clear consensus regrading which side is larger (Adibelli et al., 2011; Akgul et al., 2016; Barghouth et al., 2002; Chang et al., 2014; Dixon, 1937; Park et al., 2010; Sánchez Fernández et al., 2000; Schaeffer, 1936; Spaeth et al., 1997). There is no clear agreement regarding if sexual dimorphism exists in SS size either with some papers demonstrating larger sinuses in males while others have shown no difference (Adibelli et al., 2011; Barghouth et al., 2002; Emirzeoglu et al., 2007; Idowu et al., 2009; Karakas & Kavakli, 2005; Park et al., 2010; Sánchez Fernández et al., 2000; Spaeth et al., 1997; Vidić, 1968; Yonetsu et al., 2000).

6 | THE ETHMOIDAL CELLS

The ethmoidal cells are a quadrangular shaped, labyrinth-like structure, located between the orbit and nasal cavity consisting of multiple individuals air cells separated by thin bony walls. They are bordered laterally by the lamina papyracea, superiorly by the fovea ethmoidalis, posteriorly by the body of the sphenoid and anteriorly by the lacrimal and frontal bones (Ogle et al., 2012). These cells are divided into two groups, the anterior and posterior ethmoidal cells, by the basal lamina (Figure 4). The anterior ethmoidal cells drain into the middle meatus and can be further subdivided as cells that communicate with the frontal recess, ethmoidal infundibulum or the region of the ethmoidal bulla (Schaeffer, 1920). The posterior ethmoidal cells drain into the superior or supreme meatus, and these are generally larger and fewer in number (Terrier et al., 1985). Ethmoidal cells which extend beyond

the ethmoidal field are known as extramural cells (Weiglein et al., 1992).

6.1 | Development of ethmoidal cells

The primordial ethmoidal bulla develops by 12 weeks of gestation as a cartilaginous bulge at the lateral wall of the middle meatus (Wang & Jiang, 1997). The ethmoidal bulla then acts as the originating site of the anterior ethmoidal cells which are visible from 22 weeks of gestation (Wang & Jiang, 1997). Proliferation of the evaginating nasal epithelium fills the developing sinus by the 7th month (Monteiro & Dias, 1997; Schaeffer, 1920). The posterior ethmoidal cells begin development between weeks 16 and 20 of fetal life from the posterior aspect of the ethmoidal infundibulum (Zalzal et al., 2018). Significant variation in the size and number of ethmoidal cells exists with cadaveric studies recording between 3 and 20 cells with an average of nine in each individual (Schaeffer, 1936; Van Alyea, 1939). At birth the full number of the ethmoidal cells which an individual will have are present as small underdeveloped air cells with connective tissue bands between them (Weiglein et al., 1992; Wolf et al., 1993; Zeifer, 2000). On CT imaging the anterior ethmoidal cells generally appear well-aerated, whereas posterior air cells remain opacified, presumably either fluid-filled or under-developed (Scuderi et al., 1993). It is unclear when the sinus becomes fully aerated and opacified ethmoidal cells are relatively common throughout childhood (Diament et al., 1987).

6.2 | Size and growth of ethmoidal cells

The dimensions and volumes of the ethmoidal cells have been studied using a number of imaging modalities (Tables 7 and 8). Interpretation

TABLE 7 Previous studies that have analyzed ethmoid sinus dimensions in children

Author	Sample size (n)	Age (years)	Population	Methodology	Mean measurements for youngest age cohort (mm)			Mean measurements for oldest age cohort (mm)		
					Length	Height	Width	Length	Height	Width
Schaeffer, 1920	Not stated	0–14	USA	Cadavers	Anterior: 2 Posterior: 2 (newborn)	Anterior: 5 Posterior: 5 (newborn)	Anterior: 2 Posterior: 4 (newborn)	Anterior: 5–23 Posterior: 8–20 (age 14)	Anterior: 9–16 Posterior: 9–15 (age 14)	Anterior: 10 Posterior: 14 (age 14)
Weiglein et al., 1992	134	0–12	Austria	Dried skulls	8–12 (age 0)	5–7 (age 0)	2–3 (age 0)	24–30 (age 12)	15–20 (age 12)	8–10 (age 12)
Wolf et al., 1993	102	0–12	Austria	Dried skulls + cadavers	8–12 (newborn)	1–5 (newborn)	1–3 (newborn)	18–24 (age 4–8)	10–15 (age 4–8)	9–13 (age 4–8)
Spaeth et al., 1997	5600	0–25	Germany	CT of skulls	M: 26.33 F: 28.29 (age 3)	—	M: 8.35 F: 8.85 (age 3)	M: 40.73 F: 37.54 (age 25)	—	M: 16.58 F: 14.79 (age 25)
Sánchez Fernández et al., 2000	100 normal controls	1–88	Spain	CT	21 (age 1–5)	—	7 (age 1–5)	24 (age > 20)	—	13 (age > 20)
Adibelli et al., 2011	1452	0–18	Turkey	MRI	26.2 (age 0–2.9 mo)	6.7 (age 0–2.9 mo)	6.1 (age 0–2.9 mo)	55.2 (age 15–18)	21.9 (age 15–18)	16.4 (age 15–18)

TABLE 8 Previous studies that have analyzed volumetric growth of the ethmoid sinus in children

Author	Sample size (n)	Age (years)	Population	Methodology	Mean volumes in youngest age cohort (cm³)	Mean volumes in oldest age cohort (cm³)
Sánchez Fernández et al., 2000	100 normal controls	1–88	Spain	CT, volume calculated with trapezoidal rule	0.6 (age 1–5)	5.5 (age > 20)
Park et al., 2010	260	0–25	Korea	HRCT images (1 mm slice thickness), 3D reconstruction	0.409 (age 0)	4.462 (age 25)
Adibelli et al., 2011	1452	0–18	Turkey	MRI, sinus volume index calculated	0.25 (age 0–2.9 mo)	4.62 (age 15–18)
Rennie et al., 2017b	480	1–25	South Africa	CT (0.625–1.25 mm slice thickness), 3D reconstruction	0.7367 (R) 0.7169 (L) (Age 1–3)	4.624 (R) 4.557 (L) (Age 22–25)

however is difficult due to the generally vague descriptions of methods including whether extramural cells were included or not (Sánchez Fernández et al., 2000; Spaeth et al., 1997). One study (MRI, $n = 1452$) including extramural cells showed ES sizes of $26.2 \times 6.7 \times 6.1$ mm ($l \times h \times w$) at 0 to 3 months of age, this increased to $55.2 \times 21.9 \times 16.4$ mm at 15–18 years of age (Adibelli et al., 2011). One 3D reconstruction based study (CT, $n = 260$) found an average volume at 0 years to be 0.409 cm³, this increased to 4.462 cm³ by 25 years of age (Park et al., 2010). Adibelli et al. (MRI, $n = 1452$) utilized a simplified ellipse formula, and recorded results which were consistent with the 3D reconstructed models suggesting that the ellipsoid formula may offer a fairly accurate method of approximating ethmoidal cell volume (Adibelli et al., 2011). Left–right asymmetry of the ES has not been reported but females do tend to have ethmoidal cells 5%–10% smaller compared with males (Rennie et al., 2017b; Sánchez Fernández et al., 2000; Spaeth et al., 1997).

The ethmoidal cells have an accelerated growth rate in the early years of childhood with reports varying between 0 and 7 years depending on modality used (Park et al., 2010; Spaeth et al., 1997; Wolf et al., 1993). The ethmoidal cells are the first of the paranasal sinuses to fully develop, with the anterior ethmoidal cells reaching maturity earlier than the posterior ethmoidal cells (Park et al., 2010. Most studies report they reach adult sizes by approximately 12 years of age, other studies report growth continues until 15 or 18 years (Krmpotic-Nemanic et al., 1993; Park et al., 2010; Rennie et al., 2017b; Sánchez Fernández et al., 2000; Shah et al., 2003; Spaeth et al., 1997; Weiglein et al., 1992; Wolf et al., 1993).

7 | PATHOLOGICAL PROCESSES THAT AFFECT SINUS DEVELOPMENT

The mechanisms for paranasal sinus growth are still poorly understood. Multiple theories regarding what contributes to their development have been made - these include air flow, brain growth, muscular traction, facial structure development, eruption of permanent dentition, and cellular mechanisms including molecular adhesion and migration (Iwanaga et al., 2019; Kapusuz Gencer et al., 2013). Positive air pressure transmitted from the nasopharynx into the paranasal sinuses is thought to be fundamental to normal development and therefore any obstruction within this nasal-respiratory complex, may disrupt the normal growth process (Kucybała et al., 2017). The impact on paranasal sinus growth has been studied in a number of pathological conditions and these will be reviewed in the remainder of this article.

7.1 | Nasal septal deviation

Nasal septal deviation (NSD) is associated with increased rates of chronic otitis media in children (Atila et al., 2021). NSD is believed to negatively impact normal MS growth due to increased airway resistance reducing the amount of airflow to the sinus on the convex side (Lee & Jin, 2014). NSD is also associated with an increased prevalence of sinusitis (Kucybała et al., 2017). Very few studies have assessed MS growth in children and none have demonstrated a statistically significant difference regardless of the severity of deviation (Lee & Jin, 2014; Şentürk et al., 2015). In contrast, adult studies have reported a difference in MS volume in the deviated side in individuals with severe septal deviation (>15°) (Kalabalik & Ertas, 2018; Kapusuz Gencer et al., 2013). Another study also demonstrated significantly smaller MS volume regardless of septal deviation angle (Orhan et al., 2014). The effect of NSD on other paranasal sinuses have only been reported in adults. Ethmoidal cell volume on the ipsilateral side has been shown to decrease with increasing severity of deviation (Bayrak et al., 2018; Firat et al., 2006). No difference in frontal sinus volume in individuals with NSD regardless of the degree of deviation has been reported and although higher rates of sphenoid sinus asymmetry has been reported in individuals with NSD (80.2% vs. 50.6%) differences in volume have not been quantified (Akgul et al., 2016; Bayrak et al., 2018; Karatas et al., 2015. Overall, the effects of NSD on paranasal sinus development have not been demonstrated in children however adult studies suggest that the impact on sinus growth may become increasingly apparent with age, especially in cases of severe septal deviation.

7.2 | Choanal atresia

Choanal atresia (CA) is a congenital disorder which results in the complete obstruction of the posterior choanae and therefore blocks airflow between the nose and nasopharynx (Terzi et al., 2017). Unilateral CA is often diagnosed and treated after facial development and therefore serves as a useful model in assessing the role that air flow has in paranasal sinus development (Guimaraes et al., 2007). Cephalometric and cross sectional imaging of maxillary, sphenoid and frontal sinuses being compared with either control populations or contralateral sinus volume interestingly have not demonstrated decreased sinus volumes (Behar & Todd, 2000; Diner et al., 1986; Terzi et al., 2017). Furthermore, some studies have suggested the atretic side is either symmetrical to or even larger than the non-atretic side (Guimaraes et al., 2007; Leclerc & Leclerc, 2009). These studies suggest the absence of nasal airflow does not significantly impact the growth of the paranasal sinuses, although they are limited by small sample sizes.

7.3 | Chronic sinusitis

Chronic sinusitis in pediatric patients most commonly occurs in the maxillary and anterior ethmoidal cells (April et al., 1993). Prolonged infection and inflammation of the paranasal sinuses in thought to impair normal development and is associated with a higher incidence of maxillary sinus hypoplasia and chronic maxillary atelectasis (April et al., 1993; Sivasli et al., 2003). A number of mechanisms have been proposed for this association: 1) Chronic inflammation can result in thickened sinus walls and therefore demonstrate an acquired decrease in sinus size, 2) Chronic inflammation narrows the ethmoidal infundibulum and middle meatus, thus disrupting air flow and impairing normal pneumatization, or 3) Sinusitis is more prone to occur in an already abnormally developing maxillary sinus (Fernandes, 2004). Chronic sinusitis has been shown to significantly decrease MS volume in cross sectional imaging and subjectively decrease the extent of both FS and SS pneumatization (Ikeda et al., 1998; Kim et al., 1997; Kim et al., 2008). The thickness of the bony wall of the maxillary and ethmoidal cells has been shown to be larger compared to age-matched control groups with the duration of chronic sinusitis correlating with the thickness of the bony wall in the ethmoidal cells (Kim et al., 2008). Other studies however have reported contrary findings with either no differences in paranasal sinuses or even greater volumes in patients with chronic sinusitis with this being attributed to osteolytic erosion of the sinus wall secondary to chronic inflammation (Medina et al., 1999; Sánchez Fernández et al., 2000). Unfortunately, a number of studies did not specify the duration of sinusitis and this is known to be an important factor (Ikeda et al., 1998; Kim et al., 1997; Medina et al., 1999; Sánchez Fernández et al., 2000).

7.4 | Cystic fibrosis

Cystic fibrosis (CF) commonly results in a widespread inflammatory sinus disease due to chronic stasis of thickened mucous and poor mucociliary clearance which promotes bacterial expansion (Woodworth et al., 2007). Genetic mutations and chronic sinus infections have both been hypothesized to effect growth and explain the high rates of paranasal sinus hypoplasia in CF patients (Krzeski et al., 2001; Woodworth et al., 2007). Individuals with cystic fibrosis have underdeveloped maxillary, frontal, ethmoidal and sphenoid sinuses when compared with non-cystic fibrosis inflammatory sinus disease control groups (Eggesbo et al., 2001; Kim et al., 1997; Krzeski et al., 2001). These differences are even more pronounced when two confirmed cystic fibrosis mutations are present and also becomes more prominent with age suggesting an early arrest of pneumatization (Eggesbo et al., 2001; Kim et al., 1997). The fact that sinus development is more severely affected in CF than in chronic sinusitis is likely due to the aggressive nature of the disease that causes earlier onset of inflammatory changes and longer duration of symptoms resulting in overall, less developed paranasal sinuses.

7.5 | Cleft lip and palate

There is concern that the MS may be morphologically affected in individuals with cleft lip and palate (CLP) through either different embryological development, altered airflow or nutritional deficiencies secondary to feeding problems (Demirtas et al., 2018). Early studies using conventional radiographs and one cross sectional study found no significant differences in MS size between CLP patients and control subjects (Francis et al., 1990; Havlová et al., 1970; Hikosaka et al., 2013; Robinson et al., 1982). Three studies using CT with 3D segmentation however have demonstrated maxillary sinus volume is 7.3%–33.3% smaller in individuals with CLP compared with controls, with one also demonstrating differences between the cleft and non-cleft sides in unilateral CLP patients (Demirtas et al., 2018; de Rezende Barbosa et al., 2014; Erdur et al., 2015). Overall, there is evidence to suggest that CLP does impact the normal growth of the maxillary sinus.

8 | FESS AND SINUS DEVELOPMENT

Functional endoscopic sinus surgery has become increasingly used in the treatment of recurrent or chronic sinusitis in the pediatric population where maximal medical therapy has failed. Current literature supports FESS as a safe and effective treatment for children, however, previous animal studies and case reports raise concerns regarding the long-term impact of FESS on sinus development (Bahadir et al., 2008; Carpenter et al., 1997; Levine & Mitra, 2000; Mair et al., 1995; Malone, 1996). Altered facial growth in children has been recorded in other facial surgical procedures such as nasal septoplasty, repair of mid-facial fractures, early repair of cleft palate and the Caldwell-Luc procedure (DeFreitas & Lucente, 1998; Mair et al., 1995; Ulrich & Kessler, 1973). It therefore seems appropriate to evaluate the impact that FESS may have on sinus development.

There is a scarcity of studies assessing the long-term impact of FESS on the growth and development of the paranasal sinuses in

children with available studies generally having small sample sizes. Studies on piglets found that sinus development and facial skeletal growth was significantly reduced on the side treated by FESS, with growth reaching only 57% and 65% in the maxillary sinus and ethmoidal cells respectively (Carpenter et al., 1997; Mair et al., 1995). Human studies however have challenged the notion that it disrupts normal facial development. Quantitative anthropomorphic, plain film and cross sectional analyses as well as qualitative facial analyses for symmetry and growth in children having had FEES have demonstrated no significant differences even with 10–12 year follow-up (Bothwell et al., 2002; Sagi et al., 2015; Senior et al., 2000). Although one study demonstrated a radiological decrease in MS size of 25%, despite this there was no evidence of facial asymmetry (Kosko et al., 1996). A decrease in ethmoidal cell size after endoscopic ethmoidectomy has been reported. This is associated with a bowing of the sinus wall and is theorized to be due to a loss of structural support or post-operative scar contractures however no studies have evaluated the long-term impact of this on sinus development in children (Cunnane et al., 2009; Platt et al., 2008).

9 | CONCLUSIONS

The paranasal sinuses are complex anatomical structures which have been investigated via a number of different methods. An understanding of normal development throughout childhood enables us to better determine when pathology may be affecting the developmental process. CF is a widespread inflammatory sinus disease known to effect all of the paranasal sinuses and is associated with agenesis and hypoplasia to a more significant extent than chronic sinusitis alone. Although the effect of nasal septal deviation on sinus development has not been demonstrated in children, adult studies suggest that the impact may become increasingly apparent with age, especially in cases of severe septal deviation. Cleft lip and palate has also been shown to impact the normal growth of the maxillary sinus. FEES is becoming increasingly common surgical option in the pediatric population. Preoperative imaging is important to understand the anatomy of the individual's sinuses given the variation present in a population. An understanding of when periods of rapid paranasal sinus growth occurs is also essential. The maxillary sinus undergoes biphasic growth with a rapid phase occurring between 0 and 5 years and then constant growth beyond 8 years. The frontal sinus has a period of rapid growth between 13 and 16 years. The ethmoidal cells have a rapid growth phase between 0 and 7 years. No clear periods of increased growth have been shown for the sphenoid sinus. The long-term impact of FESS on paranasal sinus development is hard to determine and some concerns have been raised based on case reports and animal studies. Ethical considerations prevent large prospective studies being performed to image children routinely after FESS and therefore available evidence is limited. The majority of post FEES evidence shows no significant differences in objective anthropomorphic measures or subjective symmetry and when case studies have shown cross sectional evidence of a decrease in sinus size there is no discernible effect on facial symmetry.

ORCID

S. Ali Mirjalili https://orcid.org/0000-0002-1599-3573
Joshua Kirkpatrick https://orcid.org/0000-0001-9788-038X

REFERENCES

Adibelli, Z. H., Songu, M., & Adibelli, H. (2011). Paranasal sinus development in children: A magnetic resonance imaging analysis. *American Journal of Rhinology & Allergy*, 25(1), 30–35.
Akgul, M. H., Muluk, N. B., Burulday, V., & Kaya, A. (2016). Is there a relationship between sphenoid sinus types, septation and symmetry; and septal deviation? *European Archives of Oto-Rhino-Laryngology*, 273(12), 4321–4328.
Al-Bar, M., Lieberman, S. M., & Casiano, R. R. (2015). Surgical anatomy of the nose and paranasal sinuses. *Pediatric and Adult SinoNasal Disorders*, 2015, 1–25.
Amin, M. F., & Hassan, E. I. (2012). Sex identification in Egyptian population using multidetector computed tomography of the maxillary sinus. *Journal of Forensic and Legal Medicine*, 19(2), 65–69.
Anon, J. B., Ronta, M., & Zinreich, S. J. (1996). Pre-and postnatal morphogenesis of the nose and paranasal sinuses. *Anatomy of the Paranasal Sinuses*, 3–10. New York: Thieme.
Anusha, B., Baharudin, A., Philip, R., Harvinder, S., & Shaffie, B. M. (2014). Anatomical variations of the sphenoid sinus and its adjacent structures: A review of existing literature. *Surgical and Radiologic Anatomy*, 36(5), 419–427.
April, M. M., Zinreich, S. J., Baroody, F. M., & Naclerio, R. M. (1993). Coronal CT scan abnormalities in children with chronic sinusitis. *The Laryngoscope*, 103(9), 985–990.
Aslier, N. G. Y., Karabay, N., Zeybek, G., Keskinoğlu, P., Kiray, A., & Sütay, S. (2016). The classification of frontal sinus pneumatization patterns by CT-based volumetry. *Surgical and Radiologic Anatomy*, 38(8), 923–930.
Atila, E. N., Topal, K., Bulut, Y. E., Kaya, Z., & Arslan, B. (2021). Effects of nasal and paranasal sinus variations on chronic otitis media development in pediatric patients. *The Eurasian Journal of Medicine*, 53(3), 231–234.
Bahadir, O., Bahadir, A., Kosucu, P., & Livaoglu, M. (2008). The effect of maxillary sinus surgery on its development. *Acta Oto-Laryngologica*, 128(5), 551–555.
Barghouth, G., Prior, J. O., Lepori, D., Duvoisin, B., Schnyder, P., & Gudinchet, F. (2002). Paranasal sinuses in children: Size evaluation of maxillary, sphenoid, and frontal sinuses by magnetic resonance imaging and proposal of volume index percentile curves. *European Radiology*, 12(6), 1451–1458.
Bayrak, S., Ramadan, S., Öztürk, C., & Dağli, E. (Eds.). (2018). Effect of septal deviation on paranasal sinus anatomy. *KBB-Forum*, 17(3), 87–94.
Behar, P. M., & Todd, N. W. (2000). Paranasal sinus development and choanal atresia. *Archives of Otolaryngology—Head & Neck Surgery*, 126(2), 155–157.
Bhushan, B., Rychlik, K., & Schroeder, J. W., Jr. (2016). Development of the maxillary sinus in infants and children. *International Journal of Pediatric Otorhinolaryngology*, 91(2016), 146–151.
Bingham, B., Wang, R. G., Hawke, M., & Kwok, P. (1991). The embryonic development of the lateral nasal wall from 8 to 24 weeks. *The Laryngoscope*, 101(9), 992–997.
Bothwell, M. R., Piccirillo, J. F., Lusk, R. P., & Ridenour, B. D. (2002). Long-term outcome of facial growth after functional endoscopic sinus surgery. *Otolaryngology—Head and Neck Surgery*, 126(6), 628–634.
Brown, W. A., Molleson, T. I., & Chinn, S. (1984). Enlargement of the frontal sinus. *Annals of Human Biology*, 11(3), 221–226.

Carpenter, K. M., Graham, S. M., & Smith, R. J. H. (1997). Facial skeletal growth after endoscopie sinus surgery in the piglet model. *American Journal of Rhinology*, 11(3), 211–217.

Chang, C. C., Incaudo, G., & Gershwin, M. E. (2014). *Diseases of the sinuses: A comprehensive textbook of diagnosis and treatment* (2nd ed.). Springer Science and Business.

Cunnane, M. E., Platt, M., Caruso, P. A., Metson, R., & Curtin, H. D. (2009). Medialization of the lamina papyracea after endoscopic ethmoidectomy: Comparison of preprocedure and postprocedure computed tomographic scans. *Journal of Computer Assisted Tomography*, 33(1), 79–81.

Cunningham, C., Scheuer, L., & Black, S. (2016). *Developmental juvenile osteology* (2nd ed.). Academic Press.

Davis, W. B. (1918). Anatomy of the nasal accessory sinuses in infancy and childhood. *The Annals of Otology, Rhinology, and Laryngology*, 27(3), 940–967.

de Rezende Barbosa, G. L., Pimenta, L. A., Pretti, H., Golden, B. A., Roberts, J., & Drake, A. F. (2014). Difference in maxillary sinus volumes of patients with cleft lip and palate. *International Journal of Pediatric Otorhinolaryngology*, 78(12), 2234–2236.

DeFreitas, J., & Lucente, F. E. (1998). The Caldwell-luc procedure: Institutional review of 670 cases: 1975-1985. *The Laryngoscope*, 98(12), 1297–1300.

Degermenci, M., Ertekin, T., Ulger, H., Acer, N., & Coskun, A. (2016). The age-related development of maxillary sinus in children. *Journal of Craniofacial Surgery*, 27(1), 38–e44.

Demirtas, O., Kalabalik, F., Dane, A., Aktan, A. M., Ciftci, E., & Tarim, E. (2018). Does unilateral cleft lip and palate affect the maxillary sinus volume? *Cleft Palate-Craniofacial Journal*, 55(2), 168–172.

Diament, M. J., Senac, M. O., Jr., Gilsanz, V., Baker, S., Gillespie, T., & Larsson, S. (1987). Prevalence of incidental paranasal sinuses opacification in pediatric patients: A CT study. *Journal of Computer Assisted Tomography*, 11(3), 426–431.

Diner, P. A., Andrieu-Guitrancourt, J., & Dehesdin, D. (1986). Unilateral congenital choanal atresia and maxillary sinus development. *Journal of Maxillofacial Surgery*, 14(5), 285–288.

Dixon, L. V. I. I. I.,. F. W. (1937). A comparative study of the sphenoid sinus: A study of 1600 skulls. *Annals of Otology, Rhinology & Laryngology*, 46(3), 687–698.

Duque, C. S., & Casiano, R. R. (2005). Surgical anatomy and embryology of the frontal sinus. In *The frontal sinus* (pp. 21–31). Springer.

Eggesbo, H. B., Sovik, S., Dolvik, S., Eiklid, K., & Kolmannskog, F. (2001). CT characterization of developmental variations of the paranasal sinuses in cystic fibrosis. *Acta Radiologica*, 42(5), 482–493.

Ekizoglu, O. Inci, E. Hocaoglu, E. Sayin, I. Kayhan, F.T. Can, I.O. (2014). The use of maxillary sinus dimensions in gender determination: A thin-slice multidetector computed tomography assisted morphometric study. *Journal of Craniofacial Surgery*, 25(3), 957–960.

Emirzeoglu, M., Sahin, B., Bilgic, S., Celebi, M., & Uzun, A. (2007). Volumetric evaluation of the paranasal sinuses in normal subjects using computer tomography images: A stereological study. *Auris, Nasus, Larynx*, 34(2), 191–195.

Erdur, O., Ucar, F. I., Sekerci, A. E., Celikoglu, M., & Buyuk, S. K. (2015). Maxillary sinus volumes of patients with unilateral cleft lip and palate. *International Journal of Pediatric Otorhinolaryngology*, 79(10), 1741–1744.

Fernandes, C. L. (2004). Forensic ethnic identification of crania: The role of the maxillary sinus - a new approach. *American Journal of Forensic Medicine and Pathology*, 25(4), 302–313.

Firat, A. K., Miman, M. C., Firat, Y., Karakas, M., Ozturan, O., & Altinok, T. (2006). Effect of nasal septal deviation on total ethmoid cell volume. *Journal of Laryngology and Otology*, 120(3), 200–204.

Francis, P., Raman, R., Korula, P., & Korah, I. (1990). Pneumatization of the paranasal sinuses (maxillary and frontal) in cleft lip and palate. *Archives of Otolaryngology—Head & Neck Surgery*, 116(8), 920–922.

Friedman, M., Bliznikas, D., Vidyasagar, R., & Landsberg, R. (2004). Frontal sinus surgery 2004: Update of clinical anatomy and surgical techniques. *Operative Techniques in Otolaryngology—Head and Neck Surgery*, 15(1), 23–31.

Fujioka, M., & Young, L. W. (1978). The sphenoidal sinuses: Radiographic patterns of normal development and abnormal findings in infants and children. *Radiology*, 129(1), 133–136.

Gagliardi, A., Winning, T., Kaidonis, J., Hughes, T., & Townsend, G. C. (2004). Association of frontal sinus development with somatic and skeletal maturation in aboriginal Australians: A longitudinal study. *Homo: Internationale Zeitschrift fur die vergleichende Forschung am Menschen.*, 55(1–2), 39–52.

Glasier, C. M., Mallory, G. B., & Steele, R. W. (1989). Significance of opacification of the maxillary and ethmoid sinuses in infants. *The Journal of Pediatrics*, 114(1), 45–50.

Guimaraes, R. E. D. S. D., Anjos, G. C., Becker, C. G., Becker, H. M. G., Crosara, P. F. T. B., & Galvao, C. P. (2007). Absence of nasal air flow and maxillary sinus development. *Revista Brasileira de Otorrinolaringologia*, 73(2), 161–164.

Hacl, A., Costa, A. L. F., Oliveira, J. M., Tucunduva, M. J., Girondi, J. R., & Nahás-Scocate, A. C. R. (2017). Three-dimensional volumetric analysis of frontal sinus using medical software. *Journal of Forensic Radiology and Imaging*, 11, 1–5.

Hammer, G., & Rådberg, C. (1961). The sphenoidal sinus: An anatomical and roentgenologic study with reference to transsphenoid hypophysectomy. *Acta Radiologica*, 6, 401–422.

Havlová, Z., Brejcha, V., Hajnis, K., & Ruzicková, J. (1970). Development of sinus maxillaris in children with complete unilateral clefts. (age class 4-7 years). *Acta Chirurgiae Plasticae*, 12(2), 65–76.

Hikosaka, M. Nagasao, T. Ogata, H. Kaneko, T. Kishi, K. (2013). Evaluation of maxillary sinus volume in cleft alveolus patients using 3-dimensional computed tomography. *Journal of Craniofacial Surgery* 24(1),e26, e23, e26.

Hinck, V. C., & Hopkins, C. E. (1960). Concerning growth of the sphenoid sinus. *Archives of Otolaryngology*, 82(1), 62–66.

Idowu, O. E., Balogun, B. O., & Okoli, C. A. (2009). Dimensions, septation, and pattern of pneumatization of the sphenoidal sinus. *Folia Morphologica*, 68(4), 228–232.

Ikeda, A., Ikeda, M., & Komatsuzaki, A. (1998). A CT study of the course of growth of the maxillary sinus: Normal subjects and subjects with chronic sinusitis. *ORL: Journal of Oto-Rhino-Laryngology & its Related Specialties*, 60(3), 147–152.

Iwanaga, J., Wilson, C., Lachkar, S., Tomaszewski, K. A., Walocha, J. A., & Tubbs, R. S. (2019). Clinical anatomy of the maxillary sinus: Application to sinus floor augmentation. *Anatomy & Cell Biology*, 52(1), 17–24.

Jang, Y. J., & Kim, S. C. (2000). Pneumatization of the sphenoid sinus in children evaluated by magnetic resonance imaging. *American Journal of Rhinology*, 14(3), 181–185.

Jaworek-Tróć, J., Walocha, J. A., Loukas, M., Tubbs, R. S., Iwanaga, J., Zawiliński, J., Brzegowy, K., Zarzecki, J. J., Curlej-Wądrzyk, A., Kucharska, E., Burdan, F., Janda, P., & Zarzecki, M. P. (2021). Folia morphologica. *Extensive pneumatisation of the sphenoid bone: Anatomical investigation of the recesses of the sphenoid sinuses and their clinical importance*, 80(4), 935–946.

Jun, B. C., Song, S. W., Park, C. S., Lee, D. H., Cho, K. J., & Cho, J. H. (2005). The analysis of maxillary sinus aeration according to aging process; volume assessment by 3-dimensional reconstruction by high-resolutional CT scanning. *Otolaryngology—Head & Neck Surgery*, 132(3), 429–434.

Kalabalik, F., & Ertas, E. T. (2018). Investigation of maxillary sinus volume relationships with nasal septal deviation, concha bullosa, and impacted or missing teeth using cone-beam computed tomography. *Oral Radiology*, 35(3), 287–295.

Kanat, A., Yazar, U., Ozdemir, B., Coskun, Z. O., & Erdivanli, O. (2015). Frontal sinus asymmetry: Is it an effect of cranial asymmetry? X-ray

analysis of 469 normal adult human frontal sinus. *Journal of Neurosciences in Rural Practice*, 6(4), 511–514.

Kapusuz Gencer, Z., Ozkiris, M., Okur, A., Karacavus, S., & Saydam, L. (2013). The effect of nasal septal deviation on maxillary sinus volumes and development of maxillary sinusitis. *European Archives of Oto-Rhino-Laryngology*, 270(12), 3069–3073.

Karakas, S., & Kavakli, A. (2005). Morphometric examination of the paranasal sinuses and mastoid air cells using computed tomography. *Annals of Saudi Medicine*, 25(1), 41–45.

Karatas, D., Koç, A., Yüksel, F., Dogan, M., Bayram, A., & Cihan, M. C. (2015). The effect of nasal septal deviation on frontal and maxillary sinus volumes and development of sinusitis. *Journal of Craniofacial Surgery*, 26(5), 1508–1512.

Kim, D. I., Lee, U. Y., Park, S. O., Kwak, D. S., & Han, S. H. (2013). Identification using frontal sinus by three-dimensional reconstruction from computed tomography. *Journal of Forensic Sciences*, 58(1), 5–12.

Kim, G. R. (1962). A morphological study of the paranasal sinuses in Koreans. *Yonsei Medical Journal*, 3(1), 11–17.

Kim, H. J., Friedman, E. M., Sulek, M., Duncan, N. O., & McCluggage, C. (1997). Paranasal sinus development in chronic sinusitis, cystic fibrosis, and normal comparison population: A computerized tomography correlation study. *American Journal of Rhinology*, 11(4), 275–281.

Kim, H. Y., Kim, M. B., Dhong, H. J., Jung, Y. G., Min, J. Y., & Chung, S. K. (2008). Changes of maxillary sinus volume and bony thickness of the paranasal sinuses in longstanding pediatric chronic rhinosinusitis. *International Journal of Pediatric Otorhinolaryngology*, 72(1), 103–108.

Kosko, J. R., Hall, B. E., & Tunkel, D. E. (1996). Acquired maxillary sinus hypoplasia: A consequence of endoscopic sinus surgery? *The Laryngoscope*, 106(10), 1210–1213.

Krmpotic-Nemanic, J., Vinter, I., Hat, J., & Jalsovec, D. (1993). Variations of the ethmoid labyrinth and sphenoid sinus and CT imaging. *European Archives of Oto-Rhino-Laryngology*, 250(4), 209–212.

Krzeski, A., Kapiszewska-Dzedzej, D., Jakubczyk, I., Jedrusik, A., & Held-Ziolkowska, M. (2001). Extent of pathological changes in the paranasal sinuses of patients with cystic fibrosis: CT analysis. *American Journal of Rhinology*, 15(3), 207–210.

Kubal, W. S. (1998). Sinonasal anatomy. *Neuroimaging Clinics of North America*, 8(1), 143–156.

Kucybała, I., Janik, K. A., Ciuk, S., Storman, D., & Urbanik, A. (2017). Nasal septal deviation and concha bullosa–do they have an impact on maxillary sinus volumes and prevalence of maxillary sinusitis? *Polish Journal of Radiology*, 82, 126–133.

Leclerc, J. E., & Leclerc, J. T. (2009). Sphenoid sinus development in choanal atresia. *International Journal of Pediatric Otorhinolaryngology*, 73(12), 1746–1750.

Lee, D. H., & Jin, K. S. (2014). Effect of nasal septal deviation on pneumatization of the mastoid air cell system: 3D morphometric analysis of computed tomographic images in a pediatric population. *Journal of International Advanced Otology*, 10(3), 251–255.

Lee, S., Fernandez, J. W., Mahadevan, M., Tarr, G., & Mirjalili, A. (2020). Using 3D-reconstruction to analyse typical growth trends of the maxillary sinus in children. *International Journal of Pediatric Otorhinolaryngology*, 138, 110334.

Levine, S. B., & Mitra, S. (2000). Maxillary sinus involution after endoscopic sinus surgery in a child: A case report. *American Journal of Rhinology*, 14(1), 7–11.

Lorkiewicz-Muszynska, D., Kociemba, W., Rewekant, A., Sroka, A., Jonczyk-Potoczna, K., & Patelska-Banaszewska, M. (2015). Development of the maxillary sinus from birth to age 18. Postnatal growth pattern. *International Journal of Pediatric Otorhinolaryngology*, 79(9), 1393–1400.

Lund, V. J., Stammberger, H., Fokkens, W. J., Beale, T., Bernal-Sprekelsen, M., Eloy, P., Georgalas, C., Gerstenberger, C., Hellings, P., Herman, P., Hosemann, W. G., Jankowski, R., Jones, N., Jorissen, M., Leunig, A., Onerci, M., Rimmer, J., Rombaux, P., Simmen, D., … Welge-

Luessen, A. (2014). European position paper on the anatomical terminology of the internal nose and paranasal sinuses. *Rhinology. Supplement*, 24, 1–34.

Mair, E. A., Bolger, W. E., & Breisch, E. A. (1995). Sinus and facial growth after pediatric endoscopic sinus surgery. *Archives of Otolaryngology—Head & Neck Surgery*, 121(5), 547–552.

Malone, B. N. (1996). Sinus ablation after endoscopic sinus surgery. *Operative Techniques in Otolaryngology—Head and Neck Surgery*, 7(3), 278–281.

Marciniak, R., & Nizankowski, C. (1959). Metopism and its correlation with the development of the frontal sinuses; a roentgen-anatomic study. *Acta Radiologica*, 5, 343–352.

Maresh, M. M., & Washburn, A. H. (1940). Paranasal sinuses from birth to late adolescence. Clinical and roentgenographic evidence of infection. *American Journal of Diseases of Children*, 60, 841–861.

McLaughlin, R. B., Jr., Rehl, R. M., & Lanza, D. C. (2001). Clinically relevant frontal sinus anatomy and physiology. *Otolaryngologic Clinics of North America*, 34(1), 1–22.

Medina, J., Tom, L. W., Marsh, R. R., & Bilaniuk, L. T. (1999). Development of the paranasal sinuses in children with sinus disease. *American Journal of Rhinology*, 13(1), 23–26.

Monteiro, V. J., & Dias, M. P. (1997). Morphogenic mechanisms in the development of ethmoidal sinuses. *The Anatomical Record: An Official Publication of the American Association of Anatomists*, 249(1), 96–102.

Moore, K., & Ross, A. (2017). Frontal sinus development and juvenile age estimation. *Anatomical Record*, 300(9), 1609–1617.

Ogle, O. E., Weinstock, R. J., & Friedman, E. (2012). Surgical anatomy of the nasal cavity and paranasal sinuses. *Oral and Maxillofacial Surgery Clinics of North America*, 24(2), 155–166.

Orhan, I., Ormeci, T., Aydin, S., Altin, G., Urger, E., & Soylu, E. (2014). Morphometric analysis of the maxillary sinus in patients with nasal septum deviation. *European Archives of Oto-Rhino-Laryngology*, 271(4), 727–732.

Ozcan, U. A., Yıldız, M. E., Ulus, S., Turk, A., Erzen, C., & Canter, H. I. (2014). Magnetic resonance imaging evaluation of fetal maxillary sinuses. *Journal of Craniofacial Surgery*, 25(2), 363–366.

Parikh, S. R., & Brown, S. M. (2004). Image-guided frontal sinus surgery in children. *Operative Techniques in Otolaryngology—Head and Neck Surgery*, 15(1), 37–41.

Park, I. H., Song, J. S., Choi, H., Kim, T. H., Hoon, S., & Lee, S. H. (2010). Volumetric study in the development of paranasal sinuses by CT imaging in Asian: A pilot study. *International Journal of Pediatric Otorhinolaryngology*, 74(12), 1347–1350.

Platt, M. P., Cunnane, M. E., Curtin, H. D., & Metson, R. (2008). Anatomical changes of the ethmoid cavity after endoscopic sinus surgery. *The Laryngoscope*, 118(12), 2240–2244.

Prossinger, H. (2001). Sexually dimorphic ontogenetic trajectories of frontal sinus cross sections. *Collegium Antropologicum*, 25(1), 1–11.

Reittner, P., Doerfler, O., Goritschnig, T., Tillich, M., Koele, W., & Stammberger, H. (2001). Magnetic resonance imaging patterns of the development of the sphenoid sinus: A review of 800 patients. *Rhinology*, 39(3), 121–124.

Rennie, C. O., Haffajee, M. R., & Satyapal, K. S. (2017a). Shape, septa and scalloping of the maxillary sinus. *International Journal of Morphology*, 35(3), 970–978.

Rennie, C. O., Haffajee, M. R., & Satyapal, K. S. (2017b). Development of the paranasal air sinuses in a South African population utilising three dimensional (3D) reconstructed models. *European Journal of Anatomy*, 21(3), 197–209.

Rennie, C. O., Haffajee, M. R., & Satyapal, K. S. (2017c). The morphology of the sphenoid air sinus from childhood to early adulthood (1 to 25 years) utilizing 3D reconstructed images. *International Journal of Morphology*, 35(4), 1261–1269.

Robinson, H. E., Zerlin, G. K., & Passy, V. (1982). Maxillary sinus development in patients with cleft palates as compared to those with normal palates. *The Laryngoscope*, 92(2), 183–187.

Rubira-Bullen, I. R., Rubira, C. M. F., Sarmento, V. A., & Azevedo, R. A. (2010). Frontal sinus size on facial plain radiographs. *Journal of Morphological Science*, 27(2), 77–81.

Ruf, S., & Pancherz, H. (1996). Development of the frontal sinus in relation to somatic and skeletal maturity. A cephalometric roentgenographic study at puberty. *European Journal of Orthodontics*, 18(5), 491–497.

Sagi, L., Eviatar, E., Gottlieb, P., & Gavriel, H. (2015). Quantitative evaluation of facial growth in children after unilateral ESS for subperiosteal orbital abscess drainage. *International Journal of Pediatric Otorhinolaryngology*, 79(5), 690–693.

Sánchez Fernández, J. M., Anta Escuredo, J. A., Sánchez Del Rey, A., & Santaolalla Montoya, F. (2000). Morphometric study of the paranasal sinuses in normal and pathological conditions. *Acta Oto-Laryngologica*, 120(2), 273–278.

Sardi, M. L., Joosten, G. G., Pandiani, C. D., Gould, M. M., Anzelmo, M., & Ventrice, F. (2018). Frontal sinus ontogeny and covariation with bone structures in a modern human population. *Journal of Morphology*, 279(7), 871–882.

Schaeffer, J. P. (1920). *The nose, paranasal sinuses, nasolacrimal passageways, and olfactory organ in man: a genetic, developmental, and anatomico-physiological consideration*. Blakiston's Son & Company.

Schaeffer, J. P. (1936). The clinical anatomy and development of the paranasal sinuses. *Penn Medicine Journal*, 39, 395–404.

Scuderi, A. J., Harnsberger, H. R., & Boyer, R. S. (1993). Pneumatization of the paranasal sinuses: Normal features of importance to the accurate interpretation of CT scans and MR images. *American Journal of Roentgenology*, 160(5), 1101–1104.

Senior, B., Wirtschafter, A., Mai, C., Becker, C., & Belenky, W. (2000). Quatitative impact of pediatric sinus surgery on facial growth. *The Laryngoscope*, 110(11), 1866–1870.

Şentürk, M., Azgın, I., Öcal, R., Sakarya, E. U., Güler, I., & Övet, G. (2015). Volumetric analysis of the maxillary sinus in pediatric patients with nasal septal deviation. *ENT Updates*, 5(3), 107–112.

Shah, R. K., Dhingra, J. K., Carter, B. L., & Rebeiz, E. E. (2003). Paranasal sinus development: A radiographic study. *Laryngoscope*, 113(2), 205–209.

Sivasli, E., Sirikci, A., Bayazyt, Y. A., Gumusburun, E., Erbagci, H., & Bayram, M. (2003). Anatomic variations of the paranasal sinus area in pediatric patients with chronic sinusitis. *Surgical & Radiologic Anatomy*, 24(6), 400–405.

Smith, S. L., Buschang, P. H., & Dechow, P. C. (2017). Growth of the maxillary sinus in children and adolescents: A longitudinal study. *Homo*, 68(1), 51–62.

Spaeth, J., Krugelstein, U., & Schlondorff, G. (1997). The paranasal sinuses in CT-imaging: Development from birth to age 25. *International Journal of Pediatric Otorhinolaryngology*, 39(1), 25–40.

Štoković, N., Trkulja, V., Dumić-Čule, I., Čuković-Bagić, I., Lauc, T., & Vukičević, S. (2016). Sphenoid sinus types, dimensions and relationship with surrounding structures. *Annals of Anatomy*, 203, 69–76.

Szolar, D., Preidler, K., Ranner, G., Braun, H., Kugler, C., & Wolf, G. (1994). The sphenoid sinus during childhood: Establishment of normal developmental standards by MRI. *Surgical and Radiologic Anatomy*, 16(2), 193–198.

Tatlisumak, E., Asirdizer, M., Bora, A., Hekimoglu, Y., Etli, Y., & Gumus, O. (2017). The effects of gender and age on forensic personal identification from frontal sinus in a Turkish population. *Saudi Medical Journal*, 38(1), 41–47.

Tatlisumak, E., Ovali, G. Y., Asirdizer, M., Aslan, A., Ozyurt, B., & Bayindir, P. (2008). CT study on morphometry of frontal sinus. *Clinical Anatomy: The Official Journal of the American Association of Clinical Anatomists and the British Association of Clinical Anatomists*, 21(4), 287–293.

Terrier, F., Weber, W., Rüfenacht, D., & Porcellini, B. (1985). Anatomy of the ethmoid: CT, endoscopic, and macroscopic. *American Journal of Neuroradiology*, 6(1), 77–500.

Terzi, S., Dursun, E., Celiker, F. B., Celiker, M., Beyazal, M., & Ozgur, A. (2017). The effects of choanal atresia on development of the paranasal sinuses and turbinates. *Surgical & Radiologic Anatomy*, 39(10), 1143–1147.

Ulrich, K., & Kessler, L. (1973). Stomatological findings after operations of the maxillary sinus in childhood. *ORL*, 35(1), 15–18.

Vaid, S., & Vaid, N. (2015). Normal anatomy and anatomic variants of the paranasal sinuses on computed tomography. *Neuroimaging Clinics of North America*, 25(4), 527–548.

Valverde, Y., Watanabe, N., Yamaki, M., & Saito, I. (2013). The frontal sinus enlargement as an indicator of growth maturity in class III patients—A pilot study. *International Journal of Medical Science and Public Health*, 2, 451–455.

Van Alyea, O. E. (1939). Ethmoid labyrinth: Anatomic study, with consideration of the clinical significance of its structural characteristics. *Archives of Otolaryngology*, 29(6), 881–902.

Van Alyea, O. E. (1941). Sphenoid sinus: Anatomic study, with consideration of the clinical significance of the structural characteristics of the sphenoid sinus. *Archives of Otolaryngology*, 34(2), 225–253.

Vidić, B. (1968). The postnatal development of the sphenoidal sinus and its spread into the dorsum sellae and posterior clinoid processes. *The American Journal of Roentgenology, Radium Therapy, and Nuclear Medicine*, 104(1), 177–183.

Walter, W. (1933). Changes in the nasal accessory sinuses after birth. *American Medical Association*, 17(2), 197–211.

Wang, J., Bidari, S., Inoue, K., Yang, H., & Rhoton, A., Jr. (2010). Extensions of the sphenoid sinus: A new classification. *Neurosurgery*, 66(4), 797–816.

Wang, R. G., & Jiang, S. C. (1997). The embryonic development of the human ethmoid labyrinth from 8-40 weeks. *Acta Oto-Laryngologica*, 117(1), 118–122.

Wang, R. G., Jiang, S. C., & Gu, R. (1994). The cartilaginous nasal capsule and embryonic development of human paranasal sinuses. *The Journal of Otolaryngology*, 23(4), 239–243.

Weiglein, A., Anderhuber, W., & Wolf, G. (1992). Radiologic anatomy of the paranasal sinuses in the child. *Surgical & Radiologic Anatomy*, 14(4), 335–339.

Wolf, G., Anderhuber, W., & Kuhn, F. (1993). Development of the paranasal sinuses in children: Implications for paranasal sinus surgery. *Annals of Otology, Rhinology & Laryngology*, 102(9), 705–711.

Woodworth, B. A., Ahn, C., Flume, P. A., & Schlosser, R. J. (2007). The delta F508 mutation in cystic fibrosis and impact on sinus development. *American Journal of Rhinology*, 21(1), 122–127.

Yonetsu, K., Watanabe, M., & Nakamura, T. (2000). Age-related expansion and reduction in aeration of the sphenoid sinus: Volume assessment by helical CT scanning. *American Journal of Neuroradiology*, 21(1), 179–182.

Yoshino, M., Miyasaka, S., Sato, H., & Seta, S. (1987). Classification system of frontal sinus patterns by radiography. Its application to identification of unknown skeletal remains. *Forensic Science International*, 34(4), 289–299.

Yun, L. S., Kim, Y. O., Lee, S.-K., & Rah, D. K. (2011). Three-dimensional computed tomographic analysis of frontal sinus in Asians. *The Journal of Craniofacial Surgery*, 22(2), 462–467.

Zalzal, H. G., O'Brien, D. C., & Zalzal, G. H. (2018). Pediatric anatomy: Nose and sinus. *Operative Techniques in Otolaryngology—Head and Neck Surgery*, 29(2), 44–50.

Zeifer, B. (2000). Pediatric sinonasal imaging: Normal anatomy and inflammatory disease. *Neuroimaging Clinics of North America*, 10(1), 137–159.